

## Polarization variables in diffractive J/psi electroproduction at HERA

---

**Sergey Baranov**<sup>\*†</sup>

*P.N.Lebedev Institute of Physics, 53 Lenin avenue, 119991 Moscow, Russia*

*E-mail: baranov@sci.lebedev.ru*

The recent H1 and ZEUS results on the spin density matrix elements  $r_{00}^{04}$  and  $r_{1-1}^1$  are compared with theoretical calculations based on the two-gluon Pomeron model.

*Diffraction 06, International Workshop on Diffraction in High-Energy Physics*

*September 5-10, 2006*

*Adamantas, Milos island, Greece*

---

<sup>\*</sup>Speaker.

<sup>†</sup>Attendance to the conference was supported by the Organizing Committee. Not a penny was paid by P.N.Lebedev Institute of Physics.

## 1. Introduction

Recently, the H1 and ZEUS collaborations have reported [1, 2] on their measurements of diffractive electroproduction of  $J/\psi$  mesons in  $ep$  collisions at HERA. The experimental data have been collected in the kinematic range corresponding to the virtualities of the exchanged photon  $2 < Q^2 < 80 \text{ GeV}^2$ , the photon-proton center-of-mass energy  $40 < W_{\gamma p} < 160 \text{ GeV}$ , and the squared four-momentum transfer at the proton vertex  $|t| < 1.2 \text{ GeV}^2$  by the H1 collaboration, and in the kinematic range  $2 < Q^2 < 100 \text{ GeV}^2$ ,  $30 < W_{\gamma p} < 220 \text{ GeV}$ , and  $|t| < 1 \text{ GeV}^2$  by the ZEUS collaboration.

Many of the measured differential cross-sections have been compared with theoretical predictions based on the two-gluon Pomeron model [3], and a good agreement is found. However, no numerical predictions have been presented for the angular distributions  $d\sigma/d\Psi$  and  $d\sigma/d\cos\theta$ , where  $\Psi$  is the angle between the electron scattering plane and the  $J/\psi \rightarrow \mu^+\mu^-$  decay plane measured in the  $\gamma^*p$  center-of-mass frame, and  $\theta$  is the polar angle of the positive muon measured in the  $J/\psi$  rest frame. The angular distributions  $d\sigma/d\Psi$  and  $d\sigma/d\cos\theta$  are connected to the spin density matrix elements  $r_{00}^{04}$  and  $r_{1-1}^1$  and contain important information on the spin transfer from the virtual photon to  $J/\psi$  meson. In particular, these distributions must be sensitive to the spin properties of the physical object mediating the interactions, the Pomeron in our case. The goal of this contribution is to fill up the deficiency of theoretical attention to these important variables.

## 2. Theoretical framework

This study focuses on the polarization variables characterizing the process

$$e + p \rightarrow e' + p' + J/\psi, \quad (2.1)$$

where the interaction is assumed to proceed via the photon-Pomeron fusion. Our calculations are based on perturbative QCD, two-gluon Pomeron model (with so called skewed gluon distributions), and nonrelativistic bound state formalism for the formation of  $J/\psi$  meson. At the parton level, we consider the subprocess

$$\gamma^* + P \rightarrow J/\psi, \quad (2.2)$$

where the Pomeron is represented by two gluons carrying the longitudinal momentum fractions  $x_1$  and  $x_2$  with respect to the quantity  $(p_p + p'_p)/2$ , with  $p_p$  and  $p'_p$  being the momenta of the initial and scattered proton. The full gauge invariant set comprises six Feynman diagrams. The evaluation of these diagrams is straightforward and follows the standard QCD rules.

The formation of  $J/\psi$  meson is treated within the nonrelativistic bound state formalism [4]: we introduce the projection operator

$$J(^3S_1) = \not{\epsilon}_\psi (\not{p}_\psi + m_\psi) / (2m_\psi^{1/2}) \quad (2.3)$$

which guarantees the proper quantum numbers of the  $c\bar{c}$  bound system and normalise the meson formation probability to the nonrelativistic wave function at the origin of coordinate space  $|\Psi(0)|^2$ . The latter quantity is known from the  $J/\psi$  leptonic decay width [5]. This approach has already

demonstrated its validity in describing the inclusive inelastic  $J/\psi$  production at modern colliders [6, 7].

The spin density matrix of  $J/\psi$  meson is determined by the momenta  $l_1$  and  $l_2$  of the  $J/\psi \rightarrow l^+l^-$  decay leptons and is taken in the form

$$\varepsilon_\psi^\mu \varepsilon_\psi^{*\nu} = 3 (l_1^\mu l_2^\nu + l_2^\mu l_1^\nu - 2m_\psi^2 g^{\mu\nu}) / m_\psi^2 \quad (2.4)$$

(with  $m_\psi$  and  $p_\psi$  being the  $J/\psi$  mass and 4-momentum). This form is equivalent to the usual  $\varepsilon_\psi^\mu \varepsilon_\psi^{*\nu} = g^{\mu\nu} - p_\psi^\mu p_\psi^\nu / m_\psi^2$ , but is the only usable to our case, because it gives access to the kinematic variables describing the orientation of the decay plane.

The spin density matrix of the virtual photon is determined by the momenta  $p_e$  and  $p_e'$  of the initial and scattered electron and is represented in our calculations by the full lepton tensor

$$L^{\mu\nu} = 8 p_e^\mu p_e'^\nu - 4(p_e k_\gamma) g^{\mu\nu}, \quad (2.5)$$

with  $k_\gamma = p_e - p_e'$  being the virtual photon momentum. Finally, the polarization vectors of the initial gluons constituting the Pomeron are defined as explicit 4-vectors. In the frame with the  $z$ -axis oriented along the Pomeron momentum, the  $x$ ,  $y$ ,  $z$ , and  $t$  components of the gluon polarization vector are parametrized as

$$\varepsilon_g^{(x,y,z,t)} = (\cos \chi, \sin \chi, 0, 0), \quad (2.6)$$

where the angle  $\chi$  is taken at random at every generated event. This definition suits both the collinear and the  $k_t$ -factorization regimes. In the collinear approximation, the averaging over the random angle  $\chi$  stands for the averaging over transverse polarizations of the on-shell gluons. At the same time, this definition meets the usual  $k_t$ -factorization prescription [8]  $\varepsilon_g^\mu = k_{g,T}^\mu / |k_{g,T}|$ , with  $\chi$  being the azimuthal angle of the gluon transverse momentum  $k_{g,T}$ .

The evaluation of Feynman diagrams has been performed using the algebraic manipulation system FORM [9]. The gauge invariance of the matrix element  $\mathcal{M}$  of subprocess (2.2) has been explicitly tested by substituting the gluon momentum  $k_g^\mu$  for the gluon polarization vector  $\varepsilon_g^\mu$ , and, independently, by substituting the photon momentum  $k_\gamma^\mu$  for the photon polarization vector  $\varepsilon_\gamma^\mu$ .

The matrix element  $\mathcal{M}$  of the partonic subprocess (2.2) has to be convoluted with generalised (or skewed) gluon distribution  $\mathcal{H}$ . Let  $x_P$  be the Pomeron momentum fraction,  $x_1$  and  $x_2$  the gluon momentum fractions, and  $v$  and  $\xi$  the integration variables in symmetric notation [10], such that  $x_1 = (\xi + v)/(1 + \xi)$ ,  $x_2 = (\xi - v)/(1 + \xi)$ ,  $x_1 + x_2 = x_P = 2\xi/(1 + \xi)$ . Then, the amplitude of the process (2.1) reads

$$\mathcal{A}(ep \rightarrow ep\psi) = \int_{-1}^1 \frac{\mathcal{M} \mathcal{H}(v, \xi)}{(v + \xi - i\varepsilon)(v - \xi + i\varepsilon)} dv. \quad (2.7)$$

The expression for  $\mathcal{M}$  is real and has no singularities at  $v = \pm\xi$ .

In the approach which we are using here, the skewed gluon distribution  $\mathcal{H}(v, \xi)$  is related to the symmetric double distribution  $F_{DD}(x, y)$  [11] via the reduction integral

$$\mathcal{H}(v, \xi) = \int_{-1}^1 dx' \int_{-1+|x'|}^{1-|x'|} dy' \delta(x' + \xi y' - v) F_{DD}(x', y'), \quad (2.8)$$

and a model for  $F_{DD}(x, y)$  was introduced in [12], in which its functional form is factorised in the  $x$  and  $y$  and  $t$  dependence:

$$F_{DD}(x, y; \mu^2, t) = \pi(x, y) G(x, \mu^2) r(t). \quad (2.9)$$

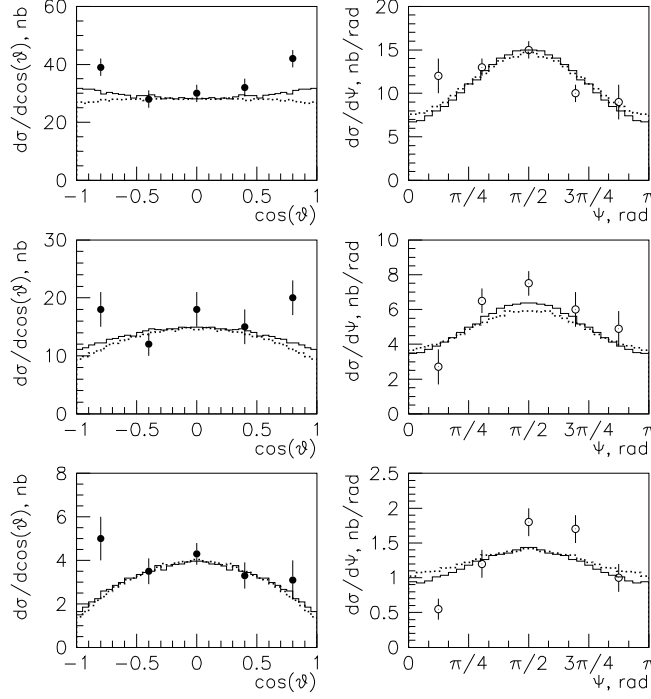


**Figure 1:** Comparison between the different  $J/\psi$  production mechanisms for three different domains of  $Q^2$  at the H1 conditions. The panels from top to bottom:  $2 < Q^2 < 5 \text{ GeV}^2$ ;  $5 < Q^2 < 10 \text{ GeV}^2$ ;  $10 < Q^2 < 80 \text{ GeV}^2$ . Solid histograms, the contribution from the two-gluon exchange; dotted histograms, the inclusive inelastic photon-gluon fusion artificially normalized to the data;  $\bullet$  and  $\circ$ , the H1 data points [1].

In accord with [13], the profile function  $\pi(x, y)$  is chosen in the form

$$\pi(x, y) = \frac{\Gamma(2b+2)}{2^{2b+1} \Gamma^2(b+1)} \frac{[(1-|x|)^2 - y^2]}{(1-|x|)^{2b+1}}, \quad (2.10)$$

normalized to  $\int_{-1+|x|}^{1-|x|} \pi(x, y) dx = 1$ , and with parameter  $b$  set equal to 2 for the case of gluons. For the input ordinary gluon density  $G(x, \mu^2)$  the Glück-Reya-Vogt (GRV) set [14] has been chosen. We have checked that the resulting parametrization is numerically very close to the one presented in Ref. [15].

### 3. Numerical results and discussion

As it follows from rather general principles [16], the angular distributions which we are considering here must have the form

$$d\sigma/d\cos\theta \propto 1 + r_{00}^{04} + (1 - 3r_{00}^{04}) \cos^2\theta \quad \text{and} \quad d\sigma/d\Psi \propto 1 - r_{1-1}^1 \cos(2\Psi). \quad (3.1)$$

In addition to that, the  $s$ -channel helicity conservation (SCHC) together with natural spin-parity exchange (NPE) hypothesis imply the following relation [16] between the spin density matrix elements:

$$r_{1-1}^1 = (1 - r_{00}^{04})/2. \quad (3.2)$$

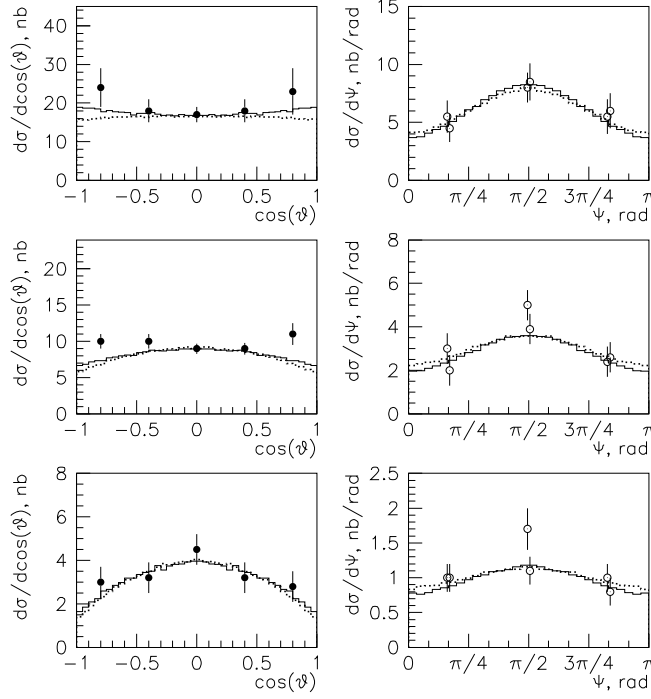


**Figure 2:** Same as Fig. 1, but for the ZEUS experimental conditions. The panels from top to bottom:  $2 < Q^2 < 5 \text{ GeV}^2$ ;  $5 < Q^2 < 10 \text{ GeV}^2$ ;  $10 < Q^2 < 100 \text{ GeV}^2$ . Notation of the curves is as in Fig. 1; ● and ○, the ZEUS data points [2].

We start with showing the H1 sample [1] in Fig. 1. There is a notable feature that the H1 data seem to disagree with SCHC and NPE expectations. As it is evident from Eq. (3.2), the distribution  $d\sigma/d\Psi$  must be more bulging when the distribution  $d\sigma/d\cos\theta$  has its wings up, and must be more flat when  $d\sigma/d\cos\theta$  has its wings down, while the experimental data show the opposite behavior.

The histograms represent our theoretical predictions. Shown there are the contributions from the two-gluon exchange mechanism and the normalized contribution from the ordinary inclusive inelastic  $J/\psi$  production via the photon-gluon fusion partonic subprocess  $\gamma^* + g \rightarrow J/\psi + g$ . In the latter case, we restrict our calculations to the same kinematic area as for the diffractive  $J/\psi$  production. This means that the usual cuts on  $Q^2$ ,  $W_{\gamma p}$ , and  $t$  are accompanied with 'diffraction selection' cuts on the  $J/\psi$  transverse momentum  $p_{\psi,T}$  in the  $\gamma^* + p$  rest frame  $p_{\psi,T}^2 < 1.2 \text{ GeV}^2$  (motivated by  $|t| < 1.2 \text{ GeV}^2$ , otherwise the momentum conservation cannot be fulfilled) and the elasticity parameter  $z = (p_\psi p_p)/(p_\gamma p_p)$ ,  $0.95 < z < 1$ , in accord with [1]. These cuts guarantee that the energy of the initial photon converts into the outgoing  $J/\psi$  meson rather than into coproduced hadronic system. Within these cuts, the inelastic photon-gluon fusion mechanism produces events which are very similar in shape to the true diffractive events. It must be kept in mind, however, that the plots presented in Fig. 1 are artificially normalized to the data (for the convenience of comparing the shapes), while the actual size of the photon-gluon fusion contribution is deficient by a significant factor (ranging from 15 at high  $Q^2$  to 40 at low  $Q^2$ ). The latter fact rules out the interpretation of diffractive events as fluctuations of inclusive inelastic events.

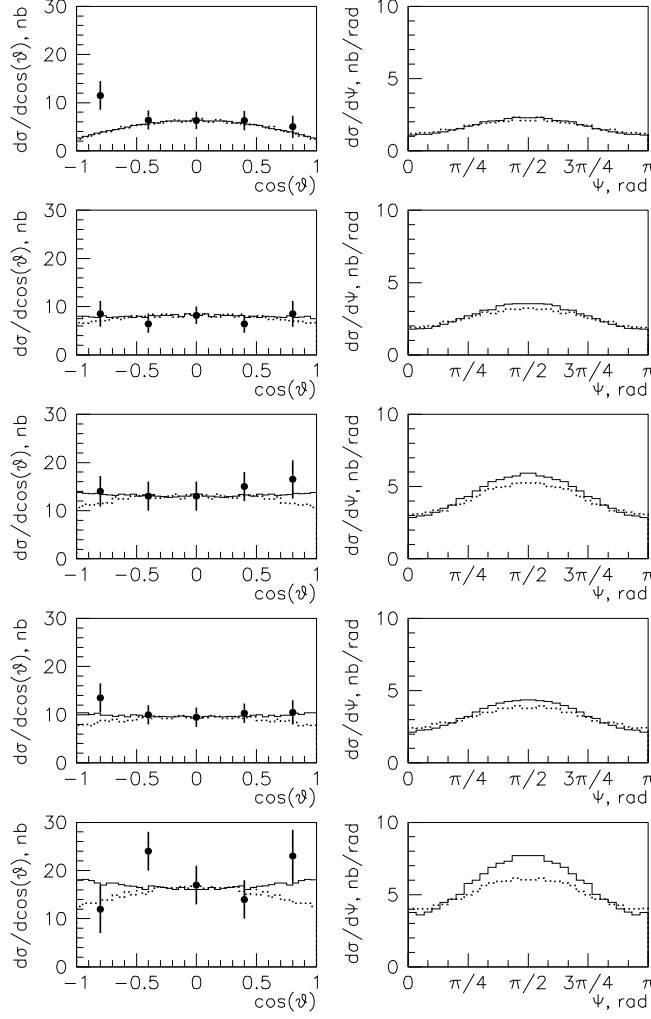


**Figure 3:** Same as Fig. 2, but for the different domains of  $W_{\gamma p}$ . The panels from top to bottom:  $30 < W_{\gamma p} < 55$  GeV;  $55 < W_{\gamma p} < 80$  GeV;  $80 < W_{\gamma p} < 120$  GeV;  $120 < W_{\gamma p} < 160$  GeV;  $160 < W_{\gamma p} < 220$  GeV; Notation of the curves is as in Figs. 1 or 2;  $\bullet$  and  $\circ$ , the ZEUS data points [2].

We proceed with showing the data collected by the collaboration ZEUS [2]. Figs. 2 and 3 display the angular distributions  $d\sigma(\gamma^* p \rightarrow \psi p)/d\cos\theta$  and  $d\sigma(\gamma^* p \rightarrow \psi p)/d\psi$  for three different domains of  $Q^2$  and five different domains of  $W_{\gamma p}$ . In all cases a more or less reasonable agreement with the theoretical predictions is found. Within the experimental errors the ZEUS data seem to be compatible with the SCHC hypothesis.

One can also notice the negative correlation between the  $Q^2$  and  $W_{\gamma p}$  bins, so that the shape of the  $d\sigma(\gamma^* p \rightarrow \psi p)/d\cos\theta$  curve seen in the highest  $Q^2$  bin resembles the one seen in the lowest  $W_{\gamma p}$  bin, and vice versa. This correlation looks rather natural in view of the kinematic relation between the  $W_{\gamma p}$  and  $Q^2$ :  $W_{\gamma p}^2 = -Q^2 + 2(k_{\gamma p}) + m_p^2$ .

## 4. Conclusion

We have considered the diffractive production of  $J/\psi$  mesons at HERA conditions and derived theoretical predictions on the angular distributions  $d\sigma(\gamma^* p \rightarrow \psi p)/d\cos\theta$  and  $d\sigma(\gamma^* p \rightarrow \psi p)/d\Psi$  in the framework of the two-gluon Pomeron model. The theoretical results have been compared with the data collected by the collaborations H1 and ZEUS. In general, a more or less reasonable agreement is found, with a few exceptions. The most important disagreement concerns the violation of the  $s$ -channel helicity conservation, which is seen in the H1 data. On the other hand, the ZEUS data seem to be compatible with this hypothesis.

Also, we have considered the inclusive inelastic  $J/\psi$  production and demonstrated that, within the diffraction cuts, the inelastic photon-gluon fusion mechanism produces events which are very similar in shape to the true diffractive events. At the same time, the absolute value of the non-diffractive contribution is insufficient to describe the data by more than one order of magnitude. Consequently, the interpretation of diffractive events as fluctuations of inclusive inelastic events is unacceptable, at least, for the particular process that we have studied.

## References

- [1] H1 Collab., A. Aktas *et al.* , Eur. Phys. J. C **46**, 585 (2006).
- [2] ZEUS Collab., S. Chekanov *et al.* , Nucl. Phys. **B695**, 3 (2004).
- [3] A. D. Martin, M. G. Ryskin, and T. Teubner, Phys. Rev. D **62**, 014022 (2000).
- [4] C.-H. Chang, Nucl. Phys. **B172**, 425 (1980); E. L. Berger and D. Jones, Phys. Rev. D **23**, 1521 (1981); R. Baier and R. Rückl, Phys. Lett. B **102**, 364 (1981); H. Krasemann, Z. Phys. C **1**, 189 (1979); G. Guberina, J. Kühn, R. Peccei, and R. Rückl, Nucl. Phys. **B174**, 317 (1980).
- [5] Particle Data Group, S. Eidelman *et al.* , Phys. Lett. B **592**, 1 (2004).
- [6] S. P. Baranov, Phys. Rev. D **66**, 114003 (2002).
- [7] S. P. Baranov and N. P. Zotov, J. Phys. G **29**, 1395 (2003); A. V. Lipatov and N. P. Zotov, Eur. Phys. J. C **27**, 87 (2003).
- [8] L. V. Gribov, E. M. Levin, and M. G. Ryskin, Phys. Rep. **100**, 1 (1983); E. M. Levin and M. G. Ryskin, Phys. Rep. **189**, 267 (1990).
- [9] J. A. M. Vermaseren, Symbolic Manipulations with FORM, published by CAN (Computer Algebra Nederland), Kruislaan 413, 1098, SJ Amsterdam 1991, ISBN 90-74116-01-9.
- [10] X. D. Ji, Phys. Rev. D **55**, 7114 (1997).
- [11] A. V. Radyushkin, Phys. Rev. D **56**, 5524 (1997).
- [12] A. V. Radyushkin, Phys. Rev. D **59**, 014030 (1999); Phys. Lett. B **449**, 81 (1999).
- [13] A. Freund, M. McDermott, and M. Strikman, Phys. Rev. D **67**, 036001 (2003).
- [14] M. Glück, E. Reya, and A. Vogt, Eur. Phys. J. C **5**, 461 (1998).
- [15] K. J. Golec-Biernat, A. D. Martin, and M. G. Ryskin, Phys. Lett. B **456**, 232 (1999).
- [16] K. Schilling and G. Wolf, Nucl. Phys. **B61**, 381 (1973).